Multi-fault mode analysis for reactor cavity cooling system of high temperature gas-cooled reactor

Zhengyang Li[1]

[1] *Institute of Nuclear and New Energy Technology, Tsinghua University, Beijing, China, 10084,*
lizhengy24@mails.tsinghua.edu.cn

EXTENDED ABSTRACT

1.Introduction

As a Generation IV reactor, the high-temperature gas-cooled reactor (HTGR) exhibits inherent safety features. A commercial-scale 200 MW- High Temperature gas-cooled Reactor Pebble-bed Module (HTR-PM) has been designed, constructed and operated in China as a demonstrate plant. In HTR-PM, a passive Reactor Cavity System (RCCS) is design to carry out the heat from the core to the final heat sink – the atmosphere, and thereby keep the safety of Reactor Pressure Vessel (RPV), the reactor cavity and the confinement in the normal operations as well in the accident conditions. Therefore, RCCS is an important safety class system for the HTGR.

The working principle of RCCS is shown in Figure 1. The water-cooling panel is installed inside the confinement and surround the RPV, vertical pipes are welded on the panel. The heat can be transferred from the RPV to the water-cooling panel via radiation and natural convection to heat up the water in the pipes. The heated water then forms the natural circulation and flows upwards to the air coolers, where the heat can be transferred from the water to the air. Finally, the heated air also forms the natural circulation and flows out of the air cooling tower. The RCCS of the HTR-PM consists of three independent cooling trains, with the design capacity of 3×50%. There is no any positive component in the RCCS, and no any further operation is needed when an accident happens and reactor shutdown is triggered, which guarantee the high reliability of this system.

Besides, an RPV support cooling system, with the same working principle as the RCCS is designed in HTR-PM. This system consists of two independent trains.

Based on the HTR-PM, a new HTR-PM600S is now under design in China, inheriting most of the design features of the HTR-PM. But in HTR-PM600S, some design optimizations were carried out, including connecting the RPV support cooling system in series to the RCCS.

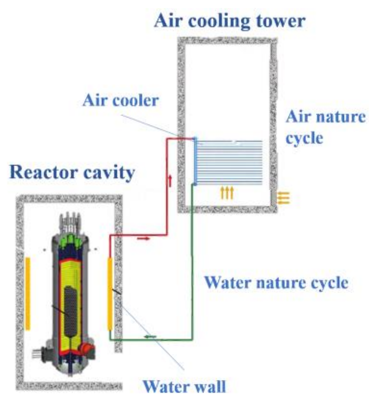

Figure 1. structure of RCCS

2.Fault modes and failure boundaries

According to the new design, the three trains of RCCS in the HTR-PM600S can be divided into two types: two trains of type A, connected with support cooling system; one train of type B, without connected with support cooling system. Thus, the fault modes of the RCCS are more complicate. In this paper, following four operation conditions of the RCCS are studied:

1) Mode1: two Type A trains and one Type B train are all operational.
2) Mode2: two Type A trains are operational.

3) Mode3: one Type A train and one Type B train are operational.
4) Mode4: one Type A train is operational.

In the RCCS, heat removal depends on natural circulation of both air and water. Therefore, successful operation requires the establishment and maintenance of natural circulation. Additionally, to prevent cavity concrete degradation and ensure the integrity of support structures, the temperature of the concrete near the RPV support must remain below a critical threshold. Three failure boundaries are defined in the program:

1) Boil boundary: The maximum water temperature must not exceed 150 °C. Boiling of water significantly reduces convective heat transfer efficiency, and is therefore considered as a system failure. This limit is based on the estimated boiling point of water at approximately 0.5 MPa.
2) Freeze boundary: The minimum temperature of the water must not fall below 0 °C, to prevent the tube crack due to freezing.
3) Support boundary: Under normal operating conditions, the temperature of the supporting concrete must not exceed 65 °C.

3.Model and equation

In order to calculate failure boundaries in different fault modes, a program based on C++ is developed. The model and equation of the program are expressed as follows.

3.1 Program Grid Division

Based on the spatial arrangement and heat transfer relationships among various modules, the system is initially divided into three sections:

1) Section 1: The gas-filled space between the reactor pressure vessel and the concrete walls of the reactor cavity. Heat transfer in this region occurs via radiation and natural convection.
2) Section 2: The water nature cycle, consisting of four modules: the water-cooled tube, the rising section of the water circuit, the air-cooled tube, and the descending section of the water circuit. Heat transfer occurs through natural convection of the cooling water.
3) Section 3: The air cooling tower, where heat transfer occurs through natural convection of air.

Section 1 and Section 2 are connected via the heat conduction module of the water-cooled wall, while Section 2 and Section 3 are linked through the heat conduction module of the air cooler. A computational model and node division, are established for the three sections and two connecting modules. The following sections provide a detailed explanation of the node divisions.

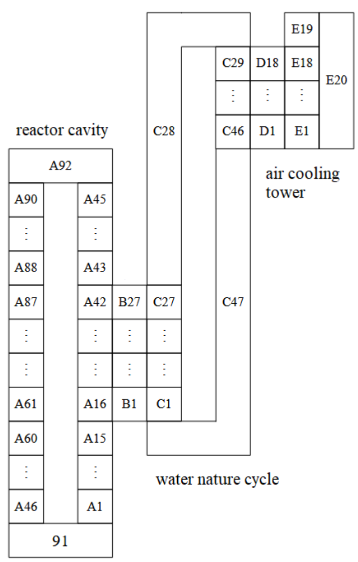

Figure 2. calculating model of RCCS

In the reactor cavity, the computational nodes are axially divided into 45 segments. The grid division is shown as figure 2. Nodes A1 to A45 correspond to the outer wall surface of the annular space, i.e., the wall surface on the water-cooled wall side. Among these, nodes A1 to A15 represent the adiabatic wall sections without steel plates, nodes A16 to A42 cover the water-cooled wall with steel plates, and nodes A43 to A45 again represent adiabatic wall sections. Nodes A46 to A90 correspond to the inner wall surface of the annular space, i.e., the outer surface of the pressure vessel. Nodes A91 and A92 represent the bottom and top surfaces of the annular space, respectively, and are assumed to be at constant temperature.

The water circulation system comprises three parts: B, C, and D. Nodes B1 to B27 represent the walls of the water-cooled tubes. Nodes C1 to C47 represent the cooling water: C1 to C27 for the water-cooled wall section, C29 to C46 for the air cooling tower, C28 for the adiabatic boundary at the rising section, and C47 for the descending section and support area. If the cooling loop is not connected to the support cooling system, only the descending section is modeled and treated as an adiabatic boundary. Nodes D1 to D18 represent the walls of the air-cooled tubes.

The air in the cooling tower is divided into 20 nodes. Nodes E1 to E20 represent the air inside the cooling tower. Node E19 is set as an adiabatic boundary, and Node E20 is set to ambient temperature.

3.2 Heat Transfer in the Reactor Cavity

Heat transfer within the cavity primarily includes two mechanisms: radiation and natural circulation between the outer wall of the pressure vessel and the water-cooled wall, and heat conduction between the water-cooled wall and the water-cooled tube walls.

The water-cooled wall, situated between the inner surface of the cavity and the outer surface of the pressure vessel, encases the upper and lower sections of the vessel. Due to the slender design of the high-temperature gas-cooled reactor's pressure vessel and the proximity of the water-cooled wall, most of the radiative heat from the pressure vessel transfers to the water-cooled wall, with a minor portion to the concrete. The temperature difference between the pressure vessel and the water-cooled wall induces air movement due to density gradients, resulting in natural convection and additional heat transfer to the water-cooled wall. Thus, the total heat transfer is the sum of natural convection and radiative heat transfer.

The outer wall of the pressure vessel and the water-cooled wall are modeled as a concentric cylindrical shell. The outer surface represents the water-cooled wall, the inner surface represents the pressure vessel, and the top and bottom surfaces represent concrete boundaries. Under steady-state conditions, the system reaches radiative equilibrium, expressed as:

$$q(S_k) = \frac{\varepsilon_k}{1-\varepsilon_k}[\sigma T^4(S_k) - J(S_k)]$$

Where:
$q(S_k)$: Radiative heat flux for surface S_k
ε_k: Emissivity of surface S_k
$J(S_k)$: Effective radiative heat flux of surface S_k

Assuming concrete is at a constant temperature of 60°C, and due to its small view factor with the steel surfaces, the error introduced by this simplification is negligible.

The heat flux density on the water-cooled wall is given by:

$$q = \frac{3\lambda\delta\left(T_{gb} - T_{sg}\right)}{b^2}$$

Each water-cooled wall includes 100 water-cooled tubes each train arranged in staggered configurations across three cooling loops to ensure uniform wall temperature under fault conditions. Heat transfer models between the water-cooled wall and the tube walls vary with the number of operational cooling loops:

Single train configuration:

$$T_{GB} = T_A + \frac{qb^2}{3\lambda\delta}$$
$$Q_A = Q_B = qb$$

Two trains configuration:

$$T_{GB} = \frac{T_A + T_B}{2} + \frac{3qb^2}{8\lambda\delta}$$
$$Q_A = 1.5qb + \frac{3\lambda\delta(T_A - T_B)}{2\text{b}}$$
$$Q_B = 1.5qb - \frac{3\lambda\delta(T_A - T_B)}{2\text{b}}$$

Three trains configuration:

$$T_{GB} = \frac{T_A}{3} + \frac{2T_B}{3} + \frac{qb^2}{8\lambda\delta}$$
$$Q_A = qb + \frac{\lambda\delta(T_A - T_B)}{\mathrm{b}}$$
$$Q_B = qb - \frac{\lambda\delta(T_A - T_B)}{2\mathrm{b}}$$

Where:

T_{GB}: Average temperature of steel plate

T_B: Water-cooled pipe surface temperature with integration into the support cooling system

T_A: Water-cooled pipe surface temperature without integration into the support cooling system

λ: Thermal conductivity of steel plate

δ: Length of the steel plate

b: Thickness of the steel plate

If two loops connected to the support cooling system fail, it is assumed that the system has failed entirely, and this condition is excluded from fault analysis.

Q_A :heat transfer density of Water-cooled pipe surface without integration into the support cooling system

Q_B: heat transfer density of Water-cooled pipe surface with integration into the support cooling system

3.3 Heat Transfer and Natural Circulation of Cooling Water

Heated by the water wall, cooling water in the tubes rises naturally, flows through the rising section into the air-cooled tubes, exchanges heat with the surrounding air, then descends back to the water-cooled tubes via the descending section, completing the loop.

Head gain from water circulation:

$$\Delta p = \sum_{29}^{47} (\rho g \Delta H)_i - \sum_{1}^{28} (\rho g \Delta H)_i$$

The equation of Flow resistance and pressure balance is shown as follows:

Frictional resistance:

$$\Delta p_1 = \sum \frac{\lambda l}{d} \frac{\rho u^2}{2}$$

Local resistance:

$$\Delta p_2 = \sum \frac{\xi \rho u^2}{2}$$

Resistance coefficient:

$$Re < 2000 \lambda = \frac{64}{\mathrm{Re}}$$
$$2000 \le \mathrm{Re} \le 4000 \lambda = 0.0025\sqrt[3]{\mathrm{Re}}$$
$$\mathrm{Re} \quad > 4000 \begin{cases} u < 11\dfrac{\nu}{K} & \lambda = \dfrac{0.3164}{\mathrm{Re}^{0.25}} \\ 11\dfrac{\nu}{K} \le u \le 445\dfrac{\nu}{K} & \lambda = 0.11\left(\dfrac{K}{d} + \dfrac{86}{\mathrm{Re}}\right) \\ u > 445\dfrac{\nu}{K} & \lambda = 0.11\left(\dfrac{K}{d}\right)^{0.25} \end{cases}$$

3.4 Heat Transfer and Natural Circulation in the Air Cooling Tower

Inside the air cooler, heated water flows upward through the tubes via natural circulation. Cooler air enters from the base of the cooling tower, and heat is transferred from the water through the tube walls to the air. Energy conservation yields the heat transfer equation:

$$T_{kg} = \frac{h_1 A_1 T_{lq} + h_2 A_2 T_{kq}}{h_1 A_1 + h_2 A_2}$$

Convective heat transfer coefficients for the inner and outer tube walls are calculated as follows:

1) Inner pipe wall:

$$Nu = 0.012 \times (\mathrm{Re}^{0.87} - 280) \times \mathrm{Pr}^{0.4} \times \left(1 + \left(\frac{d}{l}\right)^{2/3}\right)$$

Where: Nu = Nusselt number; Re = Reynolds number; Pr = Prandtl number; d = tube inner diameter; l= tube length.

2)Outer pipe wall:

$$h = 453.6u_{nf}^{0.718}$$

Where: h = convective coefficient; v = standard face velocity

Standard face velocity is determined by:

$$u_{nf} = u_F \frac{T_{nf}}{T_F} = u\cos\left(55\frac{T_{nf}}{T_F}\right)$$

Where:

u_F: Standard face velocity

u: Air velocity in the cooling tower

T_{nf}: Standard temperature (293.15 K)

T_F: Air temperature

Ambient air enters through the base louvers of the cooling tower, gets heated by the hot water in the tubes, rises due to buoyancy, and exits through the top, discharging heat to the atmosphere and completing the natural convection cycle. As shown in Figure 2, the cooling tower air nodes are divided into 19 sections (E1 to E19), with the ambient air treated as node E20, a fixed temperature boundary condition.

Buoyancy force of the air column:

$$\Delta p = (\rho g \Delta H)_{20} - \sum_{i=1}^{19} (\rho g \Delta H)_i$$

Flow resistance in the air cooler and cooling tower:

Bundle resistance in the air cooler:

$$\Delta p_1 = 5.1 N_B \phi u_{nf}^{1.504}$$

Frictional and local resistance in the cooling tower:

$$\Delta p_2 = \sum \xi \frac{\rho u^2}{2} + \sum \lambda \frac{l}{d}\frac{\rho u^2}{2}$$

4.Result and discussion

Assuming a uniform temperature distribution on the outer surface of the RPV, the failure boundaries of the RCCS under average vessel wall temperatures ranging from 100 °C to 250 °C are calculated, as shown in Figure 3.

The results indicate that all failure thresholds decline as the average outer wall temperature increases. This suggests that under higher vessel wall temperatures, the freezing threshold becomes more permissive, while the support and boiling thresholds become more restrictive. Among these four failure scenarios, fault mode 1 presents the strictest freezing boundary, while the support and boiling limits are more relaxed. fault modes 2 and 3 show similar boiling and freezing boundaries. However, since fault mode 3 involves only one Type A train, its support threshold is lower than that of fault mode 2. The figure also shows that for fault modes 1, 2, and 3, the environmental temperatures corresponding to the support and boiling thresholds all exceed 40 °C. Therefore, if at least two cooling trains are operational and the average outer wall temperature does not exceed 250 °C, neither boiling nor structural failure is expected to occur.

Subsequent analysis focuses on the freezing threshold under lower vessel temperatures and the support and boiling thresholds of fault mode 4 under higher vessel temperatures.

The figure shows that when more cooling trains are in operation, the freezing threshold rises. Under conditions where the average vessel wall temperature is 200 °C, fault mode 1 still approaches the freezing boundary. This implies that under low ambient temperatures, water freezing within the cooling towers becomes a credible risk. In fact, freezing of cooling water during winter in the air-cooling sections remains a key operational challenge for nuclear power plants.

At higher vessel temperatures, fault mode 4 shows significantly lower support and boiling thresholds. This indicates that under elevated ambient conditions, both boiling and structural failure of the support may occur. Furthermore, it is evident that at any given average vessel wall temperature, the support threshold is consistently stricter than the boiling threshold. The close alignment between the support concrete temperature and the average temperature of condensate in the support section indicates that the low support threshold in fault mode 4 primarily results from the elevated inlet water temperature.

The significance of this research is as follows:

1) This study focuses on developing a high-fidelity model and performing detailed simulations of the RCCS to demonstrate its passive reliability.
2) Using the current analysis outcomes, nuclear power plant operators can implement targeted preventive and recovery strategies—tailored to specific operating modes and accident scenarios—to ensure the RCCS remains available under defined conditions.

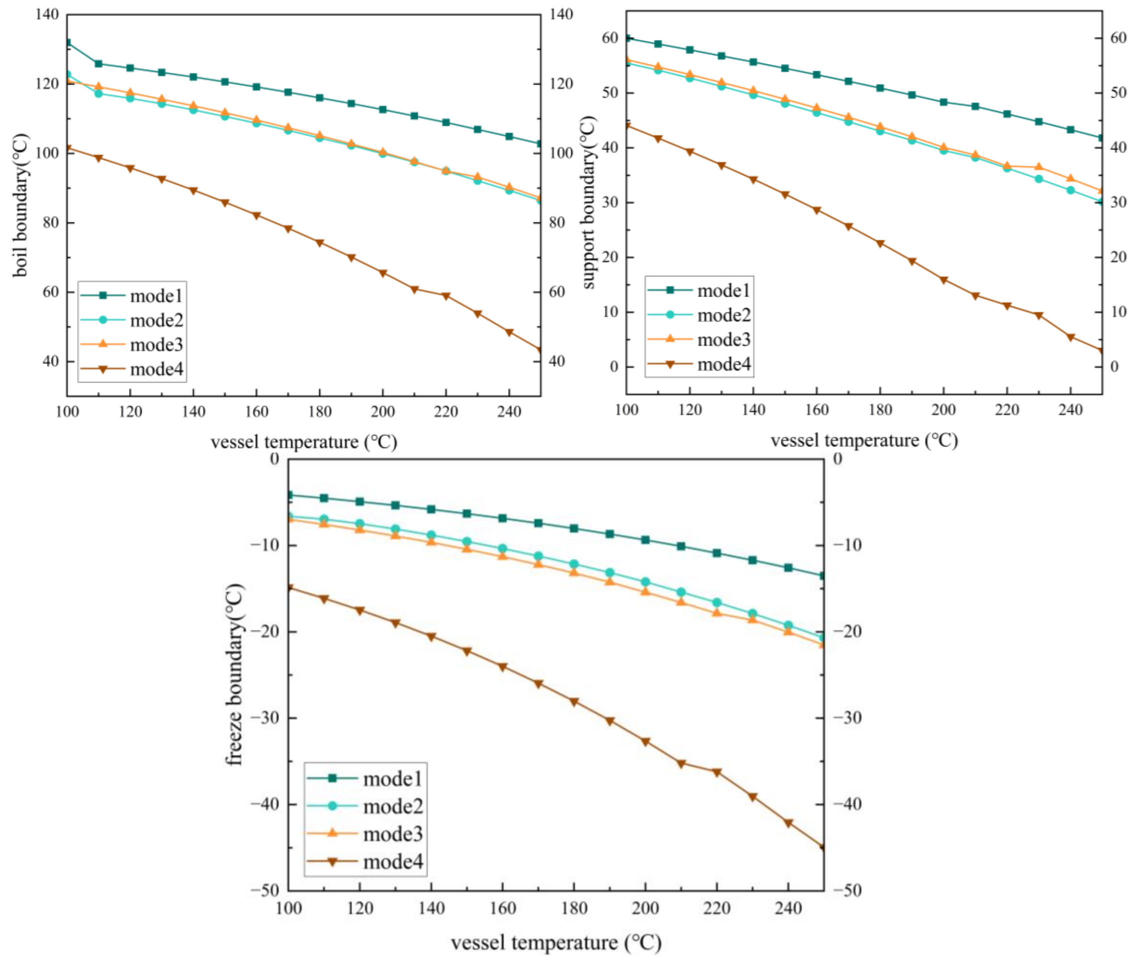

Figure 3. failure boundaries in multi-fault modes